Available online at www.sciencedirect.com

SciVerse ScienceDirect

Procedia IUTAM 00 (2014) 000–000

Procedia IUTAM

www.elsevier.com/locate/procedia

IUTAM_ABCM Symposium on Laminar Turbulent Transition

Numerical studies of non-linear intrinsic streaks in the flat plate boundary layer

Juan A. Martin[a,*], Carlos Martel[a], Pedro Paredes[a], Vassilis Theofilis[a]

[a] *Universidad Politécnica de Madrid, Pza Cardenal Cisneros 3, Madrid 28040, Spain*

Abstract

The development of streaky perturbations near the leading edge of a flat plate boundary layer was analyzed by Luchini (1996) using a description of the flow linearized around the Blaius solution. He found that there is just one single streaky mode (periodic in the spanwise direction) that grows downstream from the leading edge. The presence of this mode in the linear approximation indicates that, for the complete non-linear problem, there is an one parameter family of streak solutions that grow from the leading edge of the boundary layer. This family of steady 3D non-linear intrinsic streaks (intrinsic because they appear in the complete absence of any free stream perturbation) was recently non-linearly computed, using the Reduced Navier-Stokes formulation to describe its downstream evolution far away from the linear region. In this work, we enlarge the analysis of the transversal structure of the streaks. Furthermore, the stability characteristics of the streaky boundary-layer flow is presented using the three-dimensional Parabolized Stability Equations (PSE-3D) and spatial BiGlobal analysis formulations, which have been successfully employed in flows that are inhomogeneous in two directions and weakly dependent along the third spatial direction. The stability analysis results show that the intrinsic streaks damp Tollmien-Schlichting waves. This effect is increased as the amplitude of the streak grows. At a certain limit, as observed in linear optimal streaks, shear-layer modes become unstable, potentially producing bypass transition.

Selection and peer-review under responsibility of ABCM (Brazilian Society of Mechanical Sciences and Engineering).

Keywords: intrinsic streaks, biglobal stability analysis, PSE-3D, 3D boundary layer, reduced Navier-Stokes,

1. Introduction

Streaks are three dimensional boundary layer flow structures that take the form of spanwise thin and streamwise elongated regions of high and low speed flow that alternate in the spanwise direction. The resulting streamwise velocity profile exhibits a strong modulation in the spanwise direction, with a characteristic scale of the order of the boundary layer width (see Fig. 1).

Streaks are interesting not only for being basic flow structures developed in the flat plate boundary layer, but also for their potential to extend downstream the laminar regime of the flow, moving further the location of the transition point. The stability of the boundary layer with finite amplitude streaky distortions has been deeply analyzed[4,5,2], and experimentally tested[6,7], detecting that the increase of the amplitude of the streaks can have an stabilizing effect in the

* Corresponding author. Tel.: +34-913-366-307 ; fax: +34-913-366-307
E-mail address: juanangel.martin@upm.es

Selection and peer-review under responsibility of ABCM (Brazilian Society of Mechanical Sciences and Engineering).

Blasius boundary layer, delaying the onset of turbulence. The limit of this effect and streak stability characteristics are far from clear[1,15], and they probably depend not only on the magnitude of its spanwise modulation but also on how the streaks are generated.

This work is focused on the streaks that naturally emerge from the flat plate leading edge, without any forcing from inside the boundary layer, and in absence of any free stream perturbations. These streaks have been linearly[10,1,19,9] and non-linearly analyzed[13], and here we extend the results when the intrinsic streaks enter the non-linear regime, including an analysis of the flow stability based on the spatial BiGlobal analysis and linear PSE-3D equations.

Hydrodynamic linear stability analysis (LSA) theory considers the decomposition of all flow quantities into a base flow upon which small-amplitude perturbations are superposed. Transition prediction based on LSA using classic Linear Stability Theory (LST) and Parabolized Stability Equations (PSE) is well understood for two-dimensional or three-dimensional boundary-layers[11,8] in which the flow profiles do not depend in the spanwise direction.

When the flow problem is such that an assumption of homogeneity in two of the three spatial directions may not be made, as it is the case of a streaky boundary layer, classic LST or PSE cannot be applied. In a manner conceptually analogous to the LST, multi-dimensional linear stability theory may consider base flows which are inhomogeneous in two or three (rather than one) spatial directions. The multi-dimensional stability theories are classified in BiGlobal, PSE-3D and TriGlobal analysis; respectively, they denote analysis of base flows developing in two (BiGlobal) or three (TriGlobal) inhomogeneous spatial directions. In-between, the PSE-3D concept extends the classic PSE to flows depending strongly on two and weakly on the third spatial direction.

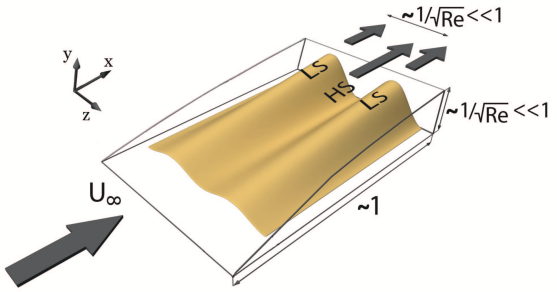

Fig. 1. Sketch of the development of a spanwise periodic array of streaks on a flat plate boundary layer, with the asymptotic scaling for $Re \gg 1$ indicated. HS (LS) stands for high (low) streamwise velocity.

2. Streak formulation

We consider a flat plate boundary layer at zero angle of incidence, with a spanwise periodic array of intrinsic steady streaks emerging from the leading edge, and developing in the streamwise direction. The formulation followed in this work is the Reduced Navier-Stokes equations (RNS).They are derived from the complete, incompressible Navier-Stokes equations with a boundary layer like approximation, in the limit of high Reynolds number. The asymptotic structure of the streaks when $Re \gg 1$ exhibits, as can be appreciated in Fig. 1, one long spatial scale in the streamwise direction, and two short spatial scales, in the wall normal and spanwise directions. These considerations lead to a system of equations fully parabolic in the streamwise direction, a detailed explanation of the resulting RNS system and of the numerical scheme used to integrate it can be followed in Martín and Martel[12], under the name of Boundary Region equations (BRE's).

In the region near the leading edge, $x \ll 1$, where the intrinsic streaks emerge, the vertical thickness of the boundary layer becomes small as compared with the spanwise period (which, for the sake of simplicity, has been set to 2π), and in first order, the flow is described by the Blasius solution. For the spanwise velocity component, a eigenvalue problem was derived and analyzed by Luchini[10], who used as starting point the linearized version of the RNS equations around the Blasius flow. The resulting two terms expansion of the solution can be expressed as

$$\overline{u} = U_{Blasius} + a x^{1-\lambda} \tilde{U}(\eta) \cos(z) + \cdots,$$

$$\begin{aligned}\bar{v} &= V_{Blasius} + ax^{1/2-\lambda}\tilde{V}(\eta)\cos(z) + \cdots, \\ \bar{w} &= -ax^{-\lambda}\left(h(\eta) - \sqrt{x}\tilde{V}(\eta) + \cdots\right)\sin(z),\end{aligned} \tag{1}$$

where $\lambda = 0.786565917\ldots$, is the first Luchini mode, which is the only eigenvalue that provides growth in x, a is a free parameter, and the profiles for $h(\eta)$, $\tilde{U}(\eta)$, and $\tilde{V}(\eta)$ are obtained in Luchini [10] and Higuera and Vega [9].

3. Stability analysis

The equations of fluid motion, the Navier-Stokes equations (NS), consist of an Initial Value Problem (IVP) for $\mathbf{q}$, which is the vector of primitive or conservative flow variables. LSA considers the decomposition of all flow quantities into a base flow, $\bar{\mathbf{q}}$, upon which small-amplitude perturbations, $\varepsilon\tilde{\mathbf{q}}$, are superposed such that $\mathbf{q} = \bar{\mathbf{q}} + \varepsilon\tilde{\mathbf{q}}$, where $\varepsilon \ll 1$. By introducing this decomposition into the equations of motion, the linearized Navier-Stokes equations (LNS) are recovered.

3.1. Spatial BiGlobal analysis

Assuming that the basic flow is dependent on two out of the three spatial coordinates, the two-dimensional parallel flow is assumed and the BiGlobal instability theory is applicable (see Theofilis [17,18] for a review).

The disturbances are three-dimensional, but a sinusoidal dependence with the homogeneous x-direction is assumed, with the periodicity length $L_x = 2\pi/\alpha$ as follows

$$\tilde{\mathbf{q}}(x,y,z,t) = \hat{\mathbf{q}}(y,z)exp[i(\alpha x - \omega t)]. \tag{2}$$

Upon substitution of the ansatz (2) in the incompressible LNS results in a two-dimensional partial derivative Generalized Eigenvalue Problem (GEVP) nonlinear on eigenvalue α, which is converted into a linear eigenvalue problem, which is larger in size by a factor equal to the degree of non-linearity (see Theofilis [16]), using the companion matrix method Bridges and Morris [3]; see Paredes [14] for more details.

3.2. PSE-3D

The PSE-3D can be derived from the three-dimensional stability equations when the basic flow can be assumed to experience slow variations along one of the three spatial directions.

Following the same reasoning made on the classical PSE [8], the PSE-3D are valid for convectively unstable flows in which the root-mean-square of the variables profiles vary slowly in the streamwise direction. The disturbance quantities are expanded in terms of their truncated Fourier components assuming that are periodic in time,

$$\tilde{\mathbf{q}}(x,y,z,t) = \sum_{n=-N}^{N} \breve{\mathbf{q}}_n(x,y,z)\exp\left[-\mathrm{i}n\omega t\right]. \tag{3}$$

Furthermore, we write $\breve{\mathbf{q}}$ as a fast varying wavy function with a slowly varying amplitude

$$\breve{\mathbf{q}}(x,y,z) = \hat{\mathbf{q}}(x,y,z)\exp\left[\mathrm{i}\int_x \alpha(x')dx'\right], \tag{4}$$

where $\hat{\mathbf{q}}(x,y,z)$ varies slowly with x.

The linear PSE-3D can be written in a compact form as:

$$\mathcal{L}\hat{\mathbf{q}} + \mathcal{M}\frac{\partial\hat{\mathbf{q}}}{\partial x} = 0, \tag{5}$$

where operators $\mathcal{L}$ and $\mathcal{M}$ act only in y and z. The entries of $\mathcal{L}$ and $\mathcal{M}$ and more details about derivation, numerical properties and solution procedure of the PSE-3D methodology are found in Paredes [14].

4. Transversal structure of intrinsic streaks

The near leading edge expressions (1) are used as initial conditions (as done in Martín and Martel [13]) for the RNS equations in order to non-linearly extend downstream the computation of the streaky flow solutions. The streaky flow has been computed for several different values of a, $a = 0.01$, $a = 0.1$, $a = 0.2$ and $a = 0.3$.

The downstream evolution of the streamwise velocity component is represented in Fig. 2. The results show that, for small values of x, the growth rate of the solutions is in very good agreement with that predicted by the expansions near leading edge (1) (marked in the plot with a thick dashed black line),but, if a is not small, nonlinear effects appear and the evolution of the maximum moves away from the linear theory predictions.

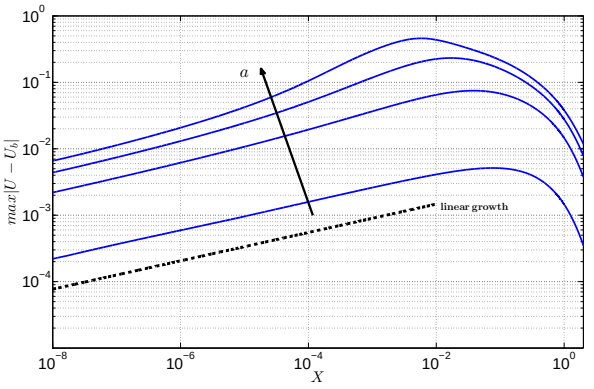

Fig. 2. Downstream evolution of maximum deviation from Blasius profile of the streamwise velocity . Solid lines: computations for $a = 0.01$, $a = 0.1$, $a = 0.2$ and $a = 0.3$, arrow indicates increasing values of a. Dashed line: asymptotic behavior of the solution near leading edge.

The transversal structure of the flow, computed in Martín and Martel [13] is shown in Fig. 3, at the downstream location where the streamwise velocity profile reaches the maximum deviation from Blasius. While the case of $a = 0.01$ (small perturbation) barely distorts the Blasius profile (left column) and the spanwise sinusoidal shape of the perturbation is retained as it evolves downstream (right column), for the higher values of a, the non-linear terms come into play and produce a very strong localization of the slow streamwise velocity region (middle column) with no longer sinusoidal shape for the perturbation.

The differences between the linear and non-linear regimes can be also observed in Fig. 4 where isosurfaces of streamwise velocity deviation from Blasius are represented, capturing the linear behavior of the structures obtained for small a, homogeneously distributed along the domain (left), and showing the strong concentration of the slow streamwise velocity into the center of the computational box, while the high streamwise velocity is spread over the domain in the case of a not small (right).

The analysis of the transversal structure of the non-linear intrinsic streaks computed is extended in Fig. 5. Colormaps of the streamwise vorticity at several x locations are plotted in columns in order to illustrate its downstream evolution, for different values of the parameter a. Note that the color scale has to be changed at each x location to properly represent the details of the vorticity field. The top vorticity plot is displayed at $x = 10^{-6}$, where it can be seen that the sinusoidal field given by the near leading edge expressions in (1) is recovered for the three values of streak intensity a.

The flow evolution for the smallest value of the perturbation, $a = 0.01$, is represented on the left column of Fig. In this case, the results show a sinusoidal spanwise shape of the vorticity that is preserved downstream with a decreasing amplitude, as the linear theory predicts. But, if the amplitude of the perturbation is not small, then the linear behavior is lost due to the effect of the nonlinear terms, as shown in the right columng of Fig. 11 for $a = 0.3$. Near the leading edge, the vorticity distribution is still given by the expressions in (1). But, away from the leading edge, this sinusoidal shape is lost, the nonlinear effects are clearly seen and the vorticity distribution becomes strongly localized near the center of the box.

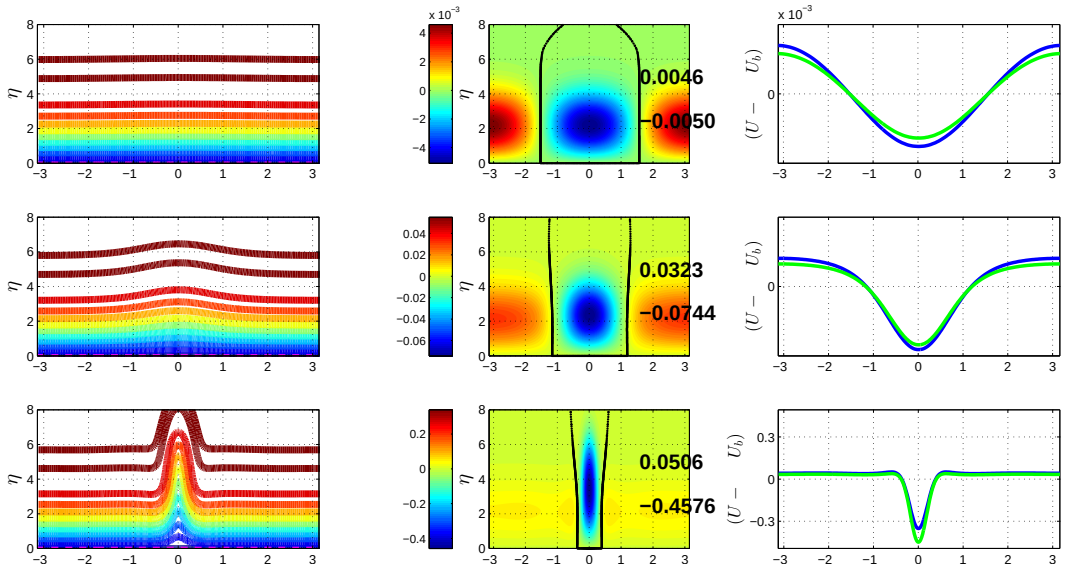

Fig. 3. Flow in transversal plane for $a = 0.01$ at $x = 7.6 \times 10^{-2}$ (top row), $a = 0.1$ at $x = 4 \times 10^{-2}$ (middle row) and $a = 0.3$ at $x = 6 \times 10^{-6}$ (bottom rown). Left column: constant streamwise contour lines for $u = 0.1, 0.2, 0.3, 0.4, 0.5, 0.6, 0.7, 0.8, 0.9$ and 0.99. Middle column: color plots of streamwise velocity deviation from Blasius profile, with the maximum and minimum values indicated. Black line denotes zero deviation. Right column: velocity deviation from Blasius in wall-normal location $\eta = 2$ ($\eta = 3$) in blue (green).

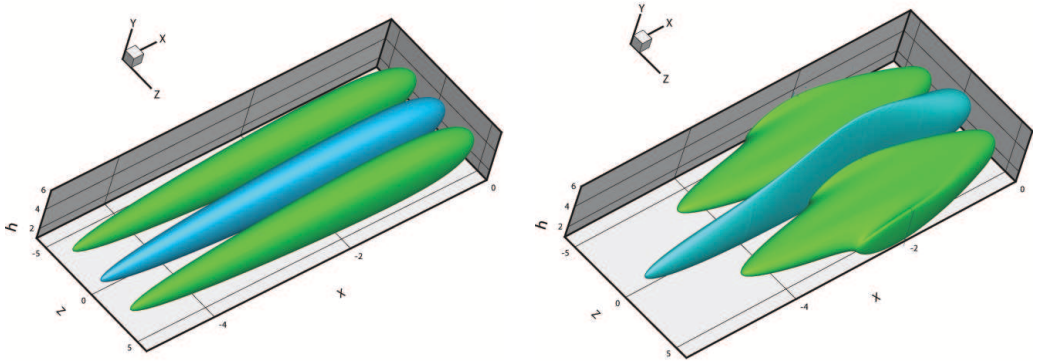

(*a*) (*b*)

Fig. 4. Isosurfaces of streamwise velocity deviation from Blasius, in (a) the value $a = 0.01$ is computed and $u - U_b = \pm 0.001$ (blue positive, green negative) represented; in (b) $a = 0.3$ and $u - U_b = \pm 0.03$ (blue positive, green negative).

This effect can be better appreciated in Fig. 6, where the isosurfaces of the streamwise vorticity are displayed. For the smallest value of a, the linear evolution is captured on the left plot, and the vorticity exhibits a homogeneous downstream evolution preserving its initial shape. The behavior changes considerably on the right plot, where the highest value of a is represented. In this case, the non-linear terms affect the development of the vorticity, concentrating its distribution into the center of the computational box.

5. Stability analysis of the intrinsic streaks

In this section, the spatial BiGlobal and PSE-3D methodologies are used to analyze the stability of the intrinsic streak flow. In Fig. 7 the neutral stability curves computed by the linear PSE-3D are displayed, corresponding to

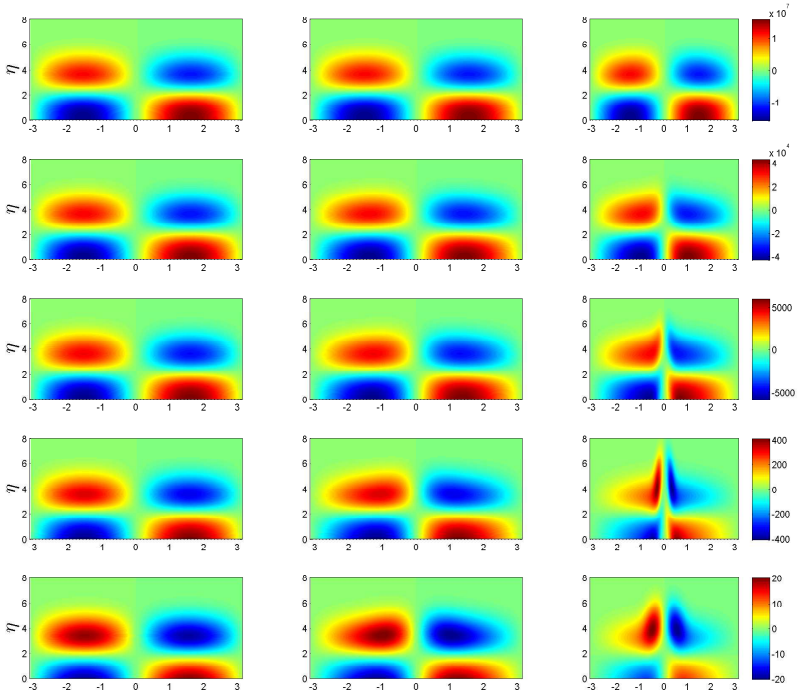

Fig. 5. Streamwise component of vorticity for $a = 0.01$ (left column), $a = 0.1$ (middle column) and $a = 0.3$ (right column) at streamwise locations, from top to bottom, $x = 1 \times 10^{-6}$, $x = 1 \times 10^{-4}$, $x = 5 \times 10^{-4}$, $x = 5 \times 10^{-3}$ and $x = 5 \times 10^{-2}$,.

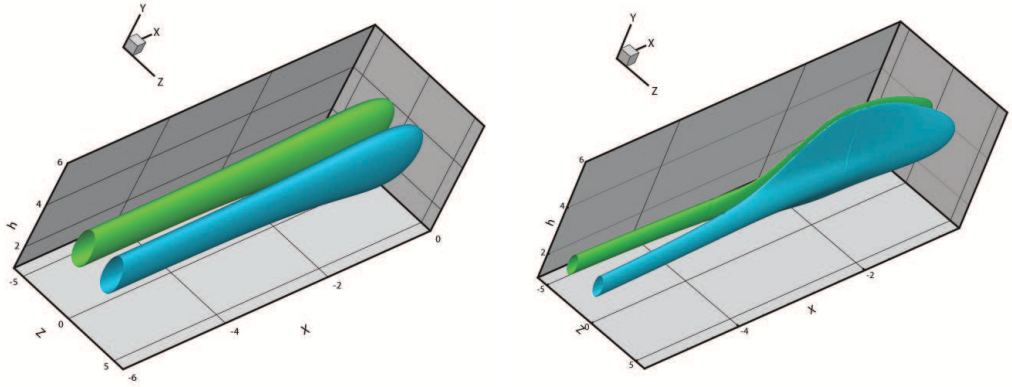

(*a*) (*b*)

Fig. 6. Isosurfaces of streamwise vorticity component, in (a) the value $a = 0.01$ is computed and $x^{0.5+\lambda}\Omega_x = 0.005 \pm 0.001$ (blue positive, green negative) represented; in (b) $a = 0.3$ and $x^{0.5+\lambda}\Omega_x = \pm 0.15$ (blue positive, green negative).

the different values of parameter a for each streak computed. The effect of damping the Tollmien-Schlichting waves is clearly observed, increasing this result with the streak intensity, which is in agreement with the previous studies performed by Cossu and Brandt[5] for linear optimal streaks. The outermost neutral curve depicted in Fig. 7 is the neutral curve of the Blasius boundary layer, while the corresponding curves for the streak amplitudes $a = 0.01$, $a = 0.1$, $a = 0.2$ and $a = 0.3$ are evenly located from the outer to the inner. It is significant to highlight that the neutral curves are plotted on a local level corresponding to a value of $Re_\delta = 500$.

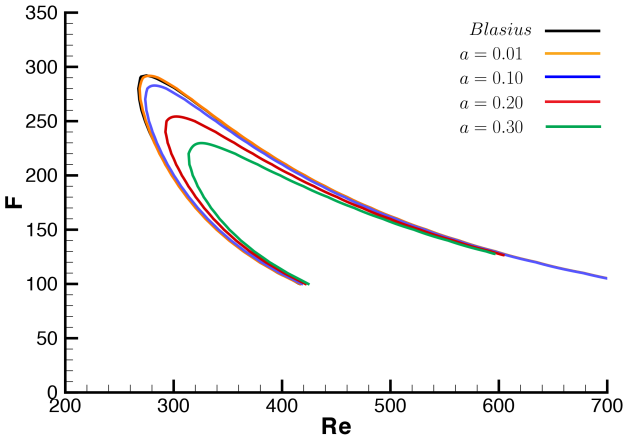

Fig. 7. Neutral stability curves for intrinsic streaks, setting $Re_\delta = 500$. Computations for Blasius flow ($a = 0$) and $a = 0.01$, $a = 0.1$, $a = 0.2$ and $a = 0.3$, increasing values of a from outer to inner.

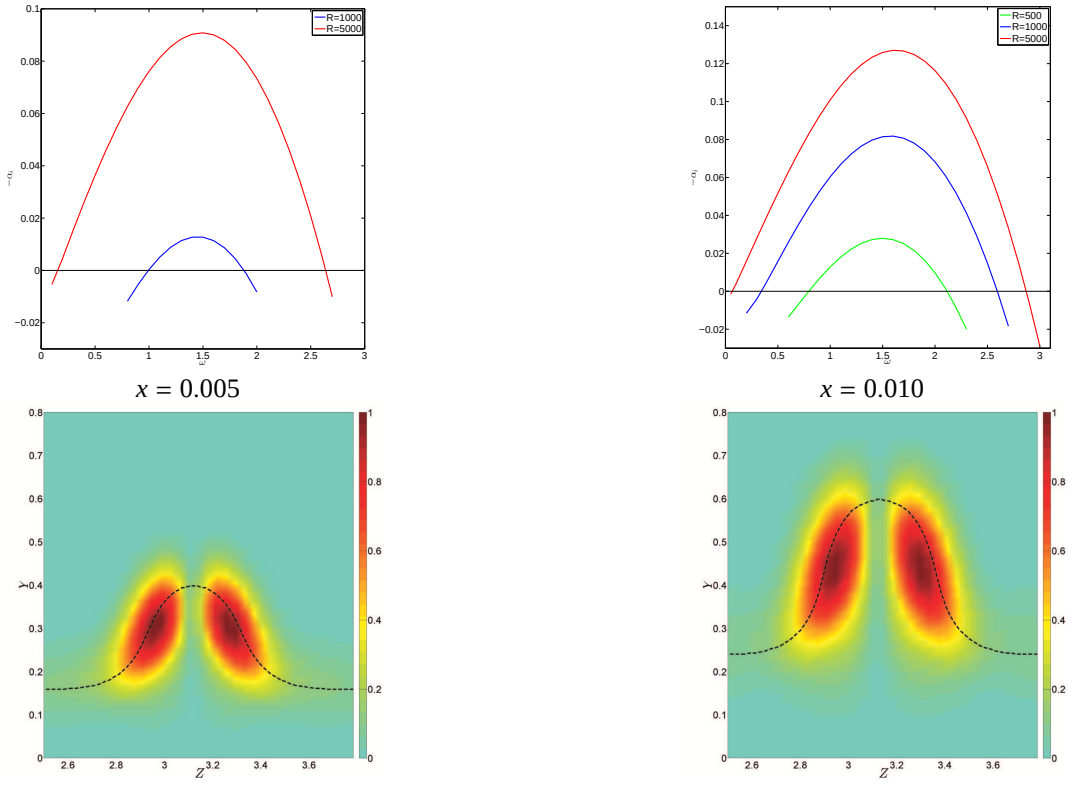

Fig. 8. Biglobal spatial stability analysis of the intrinsic streak with $a = 0.3$, at the streamwise locations $x = 0.005$ (left) and $x = 0.01$ (right). Top: growth rate curves for different Re_δ. Bottom: for $Re_\delta = 5000$ and $\omega = 1.5$, the contours of the streamwise velocity perturbation mode, depicting the critical layer with a black dash line.

Fig. 8 shows the spatial BiGlobal stability analysis at two different streamwise locations for the most intense streak, $a = 0.3$. In the top plots, the spatial growth rate is represented versus the circular frequency for different values of the Re_δ. The bottom plots display the contours of the modulus of streamwise velocity amplitude function setting $Re_\delta = 5000$ and $\omega = 1.5$. The constant value of the mean field corresponding to the phase velocity ($U = \omega/\alpha_r = 0.785$) is marked with a black dash line. It is observed that these modes peak around the critical layers, which indicates that correspond to shear-layer modes.

6. Conclusions

In this work, the one parameter family of fully non-linear intrinsic streaks that emerges from the leading edge of the flat plate is computed, showing the transversal structure of the streaky flow. The intrinsic non-linear streaks approximately consist of a narrow region of substantially slower streamwise velocity in a almost unperturbed background, and the localization and intensity of the slow streamwise velocity region increases with the amplitude of the streak.

The stabilizing effect of linear optimal streaks in Tollmien-Schlichting waves observed in computations[4,2] and experiments[6] is also demonstrated here for the intrinsic streaks. The stability of the intrinsic streaks is analyzed by means of spatial BiGlobal analysis and linear PSE-3D, recovering that the streaky flow can be more stable than the Blasius boundary layer, being this effect more intense as the amplitude of the streak is increased. For the largest initial amplitude studied, $a = 0.3$, unstable shear-layer modes are also documented, which are strongly reminiscent of the shear-layer instabilities observed in high-amplitude linear optimal streaks[4].

Acknowledgments

The work of J. A. Martín and C. Martel has been partially supported by the Spanish Ministerio de Ciencia e Innovación (grant TRA2010-18054) and by the Universidad Politécnica de Madrid (grant GI 11011039). The authors P. Paredes and V. Theofilis would like to acknowledge the support of the Spanish Ministerio de Ciencia e Innovación through Grant TRA2012-34148 (Plan Nacional 2012 - 2015).

References

1. P. Andersson, M. Berggren, and D. S. Henningson. Optimal disturbances and bypass transition in boundary layers. *Phys. Fluids*, 11(1): 134–150, 1999.
2. S. Bagheri and A. Hanifi. The stabilizing effect of streaks on Tollmien-Schlichting and oblique waves: A parametric study. *Phys. Fluids*, 19 (7):078103, 2007.
3. T.J. Bridges and P.J. Morris. Differential eigenvalue problems in which the parameter appears nonlinearly. *J. Comp. Phys.*, 55:437–460, 1984.
4. C. Cossu and L. Brandt. Stabilization of Tollmien-Schlichting waves by finite amplitude optimal streaks in the Blasius boundary layer. *Phys. Fluids*, 14(8):L57–L60, 2002.
5. C. Cossu and L. Brandt. On Tollmien-Schlichting-like waves in streaky boundary layers. *Eur. J. Mech. B. Fluids*, 23:815–833, 2004.
6. J. H. M. Fransson, L. Brandt, A. Talamelli, and C. Cossu. Experimental study of the stabilization of Tollmien-Schlichting waves by finite amplitude streaks. *Phys. Fluids*, 17(5):054110, 2005.
7. J. H. M. Fransson, A. Talamelli, L. Brandt, and C. Cossu. Delaying transition to turbulence by a passive mechanism. *Phys. Rev. Lett.*, 96: 064501–064501, 2006.
8. T. Herbert. Parabolized stability equations. *Annu. Rev. Fluid Mech.*, 29:245–283, 1997.
9. M. Higuera and J. M. Vega. Modal description of internal optimal streaks. *J. Fluid Mech.*, 626:21–31, 2009.
10. P. Luchini. Reynolds-number-independent instability of the boundary layer over a flat surface. *J. Fluid Mech.*, 327:101–115, 1996.
11. L. M. Mack. Boundary layer linear stability theory. In *AGARD–R–709 Special course on stability and transition of laminar flow*, pages 3.1–3.81, 1984.
12. J. A. Martín and C. Martel. Nonlinear streak computation using boundary region equations. *Fluid Dyn. Res.*, 44:045503, 2012.
13. J. A. Martín and C. Martel. Nonlinear intrinsic streaks in the flat plate boundary layer. *Aerosp. Sci. Technol.*, 2014. doi: http://dx.doi.org/10.1016/j.ast.2014.08.001.
14. P. Paredes. *Advances in global instability computations: from incompressible to hypersonic flow*. Phd thesis, Technical University of Madrid, 2014.
15. A. Talamelli and J.H.M. Fransson. High amplitude steady streaks in flat plate boundary layers. *AIAA paper*, 2010-4291, 2010.
16. V. Theofilis. Spatial stability of incompressible attachment line flow. *Theor. Comput. Fluid Dyn.*, 7:159–171, 1995.
17. V. Theofilis. Advances in global linear instability of nonparallel and three-dimensional flows. *Prog. Aero. Sciences*, 39 (4):249–315, 2003.
18. V. Theofilis. Global linear instability. *Annu. Rev. Fluid Mech.*, 43:319–352, 2011.
19. A. Tumin and E. Reshotko. Spatial theory of optimal disturbances in boundary layers. *Phys. Fluids*, 13:2097–2104, 2001.